Tunable Catalytic Performance of Palladium Nanoparticles for H_2O_2 Direct Synthesis via Surface-Bonded Ligands

Lucas F. de L. e Freitas[#,‡], Begoña Puértolas[×,‡], Jing Zhang[÷], Bingwen Wang[#], Adam S. Hoffman[⸸], Simon R. Bare[⸸], Javier Pérez-Ramírez[×,*], J. Will Medlin[÷,*], and Eranda Nikolla[#,*]

[#]Department of Chemical Engineering and Materials Science, Wayne State University, Detroit, Michigan 48202, United States

[×]Institute for Chemical and Bioengineering, Department of Chemistry and Applied Biosciences, ETH Zurich, Vladimir-Prelog-Weg 1, Zurich 8093, Switzerland

[÷]Department of Chemical and Biological Engineering, University of Colorado Boulder, Boulder, Colorado 80303, United States

[⸸]Stanford Synchrotron Radiation Lightsource, SLAC National Accelerator Laboratory, Menlo Park, California 94025, United States

KEYWORDS: Direct synthesis, Hydrogen peroxide, Pd-based hybrid catalysts, Surface-bonded ligands, In-situ XANES.

ABSTRACT: There is a critical need for sustainable routes to produce hydrogen peroxide, H_2O_2. A promising approach involves direct synthesis from molecular hydrogen and oxygen at (sub)ambient temperatures using unmodified supported Pd catalysts, which are limited by low selectivities. Controlling the environment of Pd active sites via surface-ligands is shown to enhance selectivity. Trends among a myriad of surface-ligands (i.e., phosphines, thiols, weakly-bound molecules) suggest that those containing H-bonding groups lead to outmost H_2O_2 production, potentially by effecting reaction energetics via H-bonding with key intermediates. These insights lay the groundwork for ligand design to achieve optimal catalyst performance for H_2O_2 synthesis.

Global demand for hydrogen peroxide (H_2O_2) has increased significantly in recent years due to its importance as an oxidant in a number of industrial processes.[1–6] H_2O_2 is commercially synthesized by the sequential hydrogenation and oxidation of anthraquinones in a mixture of organic solvents; a process challenged by high energy input, significant generation of waste, and complex liquid-liquid separations.[1–3,7] Hence, there is a critical need for developing more sustainable H_2O_2 production processes. This has led to the identification of alternative photocatalytic[4–6,8], electrocatalytic[9–12], and bioinspired routes[13–15]. Among these, the direct synthesis of H_2O_2 from molecular hydrogen (H_2) and oxygen (O_2) at (sub)ambient temperatures is an attractive approach.[16] Pd is widely used to catalyze this process, however, achieving selectivities >50% is a challenge using unmodified Pd-based catalysts, due to promotion of O-O bond activation that leads to undesired H_2O production (Scheme 1).[17,18] Several alternatives, including the use of Pd-based bimetallic catalysts, such as Pd-Au[19–32], Pd-Ag[33,34], Pd-Pt[34–37], Pd-Ru[38], Pd-Sn[21,39] and Pd-Sb[40] have been proposed to enhance H_2O_2 selectivity. However, many of these still face challenges related to the need for chemical and/or thermal treatments to effectively inhibit H_2O_2 hydrogenation, along with the high cost and toxicity introduced by the secondary metal.[9,16,40–42]

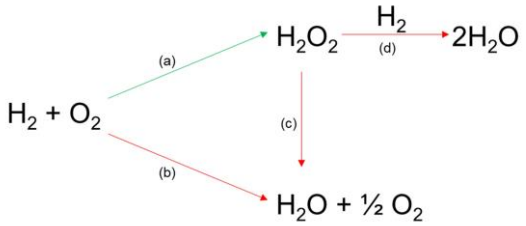

Scheme 1. Reaction pathways for: (a) formation of H_2O_2 (desired path, green) from H_2 and O_2, (b) total oxidation (red), leading to the formation of H_2O (undesired side product), (c) H_2O_2 decomposition to H_2O (red), and (d) H_2O_2 hydrogenation (red).

An approach for enhancing the H_2O_2 selectivity of Pd-based catalysts involves tuning the three-dimensional environment of the metal active sites using surface-bound ligands.[25,43–49] It has been reported that organic capping ligands, such as polyvinyl alcohol (PVA), on Pd nanoparticles (NPs) act as surface blockers to the sites that catalyze the undesired O-O bond-breaking reactions, consequently enhancing the H_2O_2 selectivity.[25] We also showed the importance of hexadecyl-2-hydroxyethyl-dimethyl ammonium dihydrogen phosphate (HHDMA) ligands bound to Pd in enhancing H_2O_2 production.[43] However, general trends

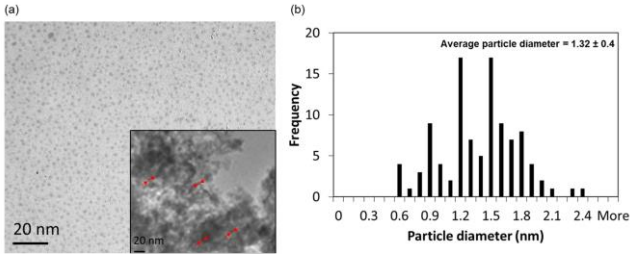

Figure 1. (a) Transmission electron micrograph (TEM) of Pd-HHDMA NPs in solution and supported on carbon (inset). (b) Histogram of the Pd particle size distribution in (a).

across various ligands to facilitate universal design strategies for optimizing metal-ligand interactions for this chemistry have not been explored.

Herein, we investigate the effect of a series of surface-bound ligands on the catalytic performance of Pd NPs supported on carbon for H_2O_2 synthesis. Activated carbon was chosen as support due to its ability to suppress side reactions.[17,50,51] We explored modification of Pd NPs with ligands using solution-based methods, and post-modification of a commercial Pd/C catalyst with self-assembled monolayers (SAMs). Pd NPs were synthesized via a colloidal method involving the reaction of sodium tetrachloropalladate(II) (Na_2PdCl_4) and HHDMA in water at 80 °C. HHDMA was used consistently for synthesizing Pd NPs to circumvent any artifacts that arise from direct synthesis of NPs using various ligands. Microscopic analysis of the synthesized Pd NPs showed an average Pd NP diameter of 1.3 ± 0.4 nm (Figure 1). The exchange of the HHDMA ligand on the Pd NP surface with a series of ligands characterized by varying binding modes and functionalities (polyethylene glycol (PEG), hexadecyltrimethylammonium bromide (CTAB), mercaptosuccinic acid (MSA), oleylamine (OAm), trioctylphosphine (TOP), see Chart S1) was achieved using two approaches: (i) a concentration gradient approach for exchanging HHDMA with hydrophilic ligands, such as PEG (Pd-PEG), CTAB (Pd-CTAB) and MSA (Pd-MSA), and (ii) a phase exchange approach for hydrophilic ligands, such as TOP (Pd-TOP) and OAm (Pd-OAm) (Supporting Information). Ligand exchange was confirmed using attenuated total reflectance Fourier transform infrared (ATR-FTIR) studies (Figure S1). H_2/D_2 scrambling experiments were used as a relative measure of the active Pd surface area for H_2 dissociation on the catalysts. The apparent rates for H_2/D_2 exchange are shown in Table S1. The highest rate was observed for carbon-supported Pd-PEG followed by Pd-HHDMA, Pd-MSA and Pd-TOP. Given the similarity in the Pd NP size for all systems, variations in the available surface area of Pd for H_2 dissociation could be associated with the difference in the ligand coverage on the Pd NP surface. This was supported by X-ray photoelectron spectroscopy (XPS) studies, which showed that the ratio of P-containing ligand to Pd (P/Pd) for carbon-supported Pd-TOP (0.15) was higher than that for carbon-supported Pd-HHDMA (0.11) (Table S2 and Figure S2).

Catalytic data of carbon-supported Pd NPs modified with various ligands (TOP, OAm, MSA, HHDMA, PEG, CTAB) are shown in Figure 2 and Table S3. The H_2O_2 production rate for all catalysts followed the same order as the rates of H_2/D_2 exchange, suggesting that the active sites for gas-phase H_2 dissociation might be similar to those required for the same process in H_2O_2 synthesis (Figure S3). The best catalytic performance was observed for carbon-supported Pd NPs capped with HHDMA, PEG, and MSA. We previously reported that the high selectivity of Pd-HHDMA based catalysts stemmed from (i) steric hindrance induced by the long ligand chain, and (ii) the strong adsorption of $H_2PO_4^-$ on the Pd surface eliminating O-O bond-breaking leading to side reactions.[43] While these factors might be important for Pd-HHDMA, they do not explain the remarkable performance of Pd-PEG and Pd-MSA, since these ligands are characterized by different chain lengths and binding modes to the Pd surface. One common characteristic among the most selective ligands is related to the OH functionality in their structure (Chart S1), which promotes hydrogenation of the OOH intermediate to H_2O_2, as opposed to O-O bond-breaking leading to H_2O production. The mechanism by which this occurs could be similar to the solvent effects reported by Wilson and Flaherty[18], who showed that H-bonding between the solvent molecules and the OOH and H_2O_2 surface species selectively promoted H_2O_2 production. In the case of the ligands without OH functionality, we observed an increase in the rate for H_2O_2 production that scaled with the bulkiness of the ligands (TOP > OAm > CTAB), suggesting a potential effect induced from steric hindrance arising from the ligands.

It is generally reported that hydrogen interaction with the Pd surface plays a key role in direct H_2O_2 synthesis.[52] To probe this interaction, we analyzed the Pd L_3-edge X-ray absorption near-edge structure (XANES) on Pd-HHDMA/C, Pd-PEG/C, P-TOP/C under He and after exposure to 10 vol% H_2/He at room temperature. While these conditions are not the same as those for H_2O_2 synthesis, they provide insights regarding changes in hydrogen-Pd-surface interactions induced by modifications with various ligands. Figure S4 shows the Pd L_3-edge XANES of supported Pd catalysts with various ligands under He and H_2 atmospheres. Upon exposure to H_2, a broad peak at 3181 eV appears for Pd-HHDMA/C and Pd-PEG/C along with a decrease in the intensity of the white line height of the main Pd L_3 edge (Figure S4); while no changes were observed for Pd-TOP/C. The decrease in the intensity of the white line of Pd L_3 edge for Pd-HHDMA/C and Pd-PEG/C is mainly due to the reduction of any oxidic Pd under H_2.[53] The broad peak at 3181 eV is associated with the formation of Pd hydride (PdH_x), which results from the mixing of the hydrogen 1s orbital with the electronic states of Pd, forming new Pd states above the Fermi level.[54] The intensity of the hydride peak in Pd catalysts has been previously related to differences in Pd particle size or surface characteristics.[52–57] Given that all the catalysts analyzed have the same particle size distribution, we assign the variations in the PdH_x peak intensity to Pd surface-ligand interactions. Furthermore, Pd NP size in these catalysts is <2.6 nm, suggesting that α-phase Pd hydride is dominant.[55] The extent of α-phase hydride formation in Pd catalysts has been reported to impact on H_2O_2 selectivity.[52] Figure 3a shows the difference spectra at the Pd L_3 edge (obtained by subtracting the spectra in He and H_2) for all catalysts, highlighting differences in the extent of PdH_x formation as a function of Pd catalysts with various ligands. A correlation between the intensity of the PdH_x peak and H_2O_2

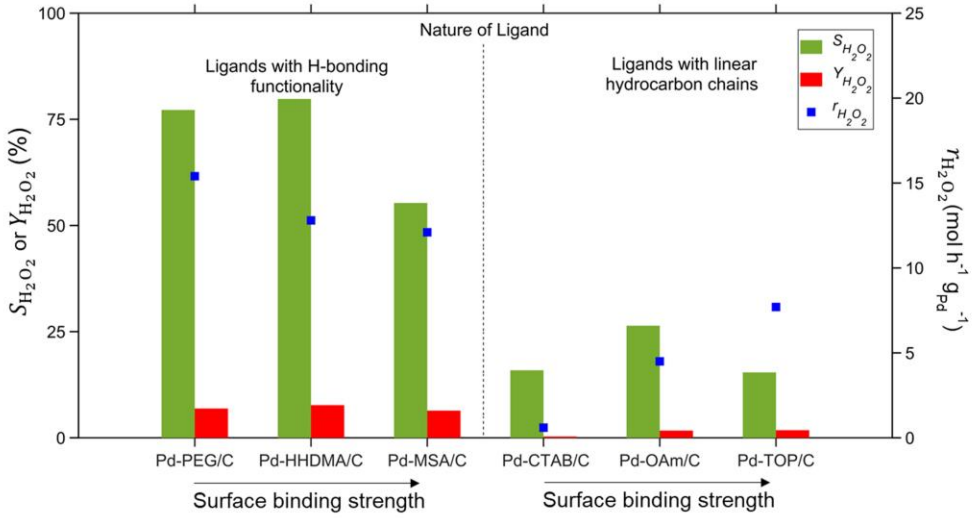

Figure 2. Catalytic performance (selectivity ($S_{H_2O_2}$), yield ($Y_{H_2O_2}$) and rate ($r_{H_2O_2}$) of H_2O_2 production) of Pd NPs with various ligands supported on activated carbon. Reaction conditions: *T*= 0 °C, *P*= 40 bar, 3.75 vol% H_2; 7.5 vol% O_2; 88.75 vol% N_2, m_{cat}= 10 mg in 5 mL of 67 vol% methanol in water. Standard deviation based on 3 independent repetitions was estimated as ±10% and ±4% for the rate of H_2O_2 production and selectivity, respectively.

selectivity of these catalysts is observed (Figure 3b). Interestingly, supported Pd NPs with surface-bound ligands (Pd-HHDMA/C and Pd-PEG/C) characterized by OH functionality were found to exhibit the highest PdH_x formation and H_2O_2 selectivity. While it is unclear if and how ligand OH functionality effects PdH_x formation, it is obvious that both of these characteristics are linked to high H_2O_2 selectivity.

To expand the window of surface modifiers, impregnation of a commercial 1 wt% Pd/C catalyst with a variety of organic molecules tailored across a wide range of functional group chemistries (i.e., phosphonic acid (PA) and thiol modifiers (Chart 1)) was used. Impregnation of commercial 1 wt% Pd/C had a significant ligand-dependent impact on the H_2O_2 selectivity (Table 1). Adamantanethiol (AT)-modified

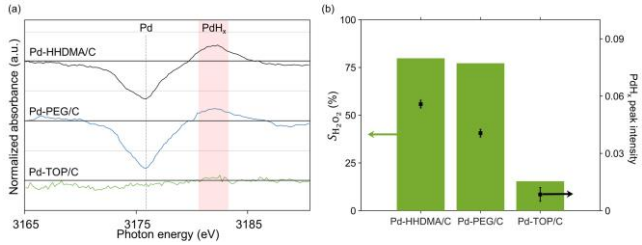

Figure 3. (a) Pd L_3-edge difference spectra for Pd/C obtained by subtracting the spectra for Pd/C in 10 vol% H_2/He from those in pure He. (b) PdH_x peak intensity in (a) along with H_2O_2 selectivity ($S_{H_2O_2}$) for Pd catalysts with various ligands. Reaction conditions: *T*= 0 °C, *P*= 40 bar, 3.75 vol% H_2; 7.5 vol% O_2; 88.75 vol% N_2, m_{cat}= 10 mg in 5 mL of 67 vol% methanol in water.

catalysts exhibited the lowest H_2O_2 selectivities. AT is known to saturate at approximately half the coverage of 1-hexanethiol (C_6SH),[58] indicating that H_2O_2 synthesis is sensitive to thiol attachment density. The observation that the increase in monolayer density profoundly affects reaction selectivity is similar to previous reports on hydrodeoxygenation catalysis.[59] In contrast to those prior studies, however, the improved selectivity does not appear to result merely from selective poisoning of Pd ensembles; in addition to the rate of H_2O formation decreasing, the rate of H_2O_2 formation increased. Whereas the former effect would be expected if high ligand densities suppress O-O activation reactions, the latter hints that the organic ligands may facilitate proton transfer to adsorbed O_2-derived intermediates.[18]

Among the thiols, thioglycerol (TG) modification led to the highest selectivity, perhaps signaling that H-bonding groups located near the surface led to enhanced H_2O_2 synthesis performance. Because TG has been found to saturate at a similar ~1/3 monolayer coverage to C_6SH on Pd[60], it is likely that the enhanced selectivity is attributable to H-bonding interactions involving the ligand tail. Flaherty and coworkers have recently reported that hydroxylated organic surface intermediates can promote proton transfer to molecular oxygen, accelerating direct H_2O_2 synthesis.[61] Similar observations were made for the PA modifiers, which also improved selectivity to varying extents. Recent work has suggested that saturation PA coverage on Pd is 2-3 nm^{-2}, and that these species can selectively promote reactions involving hydroxylated intermediates.[62] Again, a more hydrophilic PA (aminomethylphosphonic acid, NH_2MPA) capable of H-bonding interactions showed greater promotion of selectivity compared to its chloromethylphosphonic acid (ClMPA) counterpart, similar to the promotion effect of the hydrophilic TG (Figure S5). Overall, the results with the modified samples showed that tuning of the ligand identity and density provides a rich area for tuning H_2O_2 performance. Clearly, the ligand coverage is critical to selectivity promotion, while tuning interactions of the tail with reactive intermediates on the surface offers another possible route for promoting selectivity.

For the thiol and phosphonate ligands, there was no clear correlation between the rate of H_2O_2 production and the rate of HD dissociation. It is important to note that these two experiments were conducted under different conditions in the liquid versus gas-phase, which may influence ligand structure; this could be particularly important for hydrophilic modifiers like TG.[60] Notably, TG SAMs strongly

Table 1. Post-synthetic modification of Pd/C catalysts using self-assembled monolayers (SAMs) of various ligands on commercial 1 wt% Pd/C (Sigma-Aldrich). Uncertainties in r_{HD} indicate standard deviation of triplicate runs.

	$r_{H_2O_2}$ (mol h^{-1} g$_{Pd}^{-1}$)	X_{H_2} (%)	$S_{H_2O_2}$ (%)	$Y_{H_2O_2}$ (%)	r_{H_2O} (mol h^{-1} g$_{Pd}^{-1}$)	r_{HD} (mol h^{-1} g$_{Pd}^{-1}$)
Pd/C (Sigma-Aldrich)	0.5	7.7	6.5	0.5	7.2	234.2 ± 14.9
C_6SH-Pd/C	2.1	12.9	55.9	7.2	1.7	1.6 ± 0.1
TG-Pd/C	3.1	13.3	70.7	9.4	1.3	0.2 ± 0.1
AT-Pd/C	0.7	22.1	24.0	5.3	2.2	6.0 ± 0.1
BZPA-Pd/C	3.5	19.0	56.2	10.7	2.7	14.4 ± 0.4
CIMPA-Pd/C	3.1	21.2	47.5	10.1	3.4	15.4 ± 0.7
NH_2MPA-Pd/C	1.4	12.3	56.0	6.9	1.1	123.4 ± 3.4

suppressed the rate of H-D dissociation but did not have a comparable effect for H_2O_2 or water formation. While it is not immediately clear why the correlation is not observed in the case of the post-modified samples, it is worth noting that for many of these surfaces the ligand coverage is highly dense[63], potentially creating a very different microenvironment (and electronic structure) compared to the case of NPs synthesized with ligands such as PEG, HHDMA, and MSA.

In conclusion, a wide range of surface-bound ligands with varying functionalities were used to gain an understanding of the ligand characteristics that governed modulation of Pd catalyst performance for direct H_2O_2 synthesis. In general, ligands improved selectivity of supported Pd catalysts, with the ones containing H-bonding groups resulting in the highest selectivities (75-80%). These ligands were hypothesized to interact via hydrogen bonding with key reaction intermediates (i.e., OOH and adsorbed H_2O_2)[18] favoring the energetics associated withthe desired path leading to H_2O_2 production. For a subset of ligand-modified Pd catalysts, we also showed that the ones characterized by H-bonding groups led to PdH_x formation when exposed to H_2 at room temperature, uncovering another feature that potentially played a role in selectivity enhancement. We note that other mechanisms, such as the selective poisoning of sites for O_2 dissociation by groups on the ligands, cannot be ruled out. The insights obtained from these studies set the basis for designing optimal surface-bound ligands on Pd catalysts to achieve outmost catalyst performance for H_2O_2 synthesis.

ASSOCIATED CONTENT

Supporting Information. Detailed experimental methods and additional catalyst characterization (ATR-FTIR, Pd L_3-edge XANES, and XPS) are included. This material is available free of charge via the Internet at http://pubs.acs.org.

AUTHOR INFORMATION

Corresponding Author

*E-mail: erandan@wayne.edu (E. Nikolla)
*E-mail: medlin@colorado.edu (J. Will Medlin)
*E-mail: jpr@chem.ethz.ch (J. Pérez-Ramírez)

Author Contributions

The manuscript was written through contributions of all authors. / All authors have given approval to the final version of the manuscript. / ‡These authors contributed equally.

ACKNOWLEDGMENT

The authors acknowledge support from the National Science Foundation for funding this research through CHE Grant No. 1900176. We also thank the Lumigen Instrument Center at Wayne State University for the use of the X-ray diffraction/spectroscopy (National Science Foundation MRI-1427926, MRI-1849578), electron microscopy facilities (National Science Foundation MRI-0216084). Part of this work was also performed at Stanford Synchrotron Radiation Lightsource (SSRL) of SLAC National Accelerator Laboratory, and the user of the SSRL is supported by the U.S. Department of Energy, Office of Science, Office of Basic Energy Sciences under Contract No. DE-AC02-76SF00515 and by Co-ACCESS supported by the U.S. Department of Energy, Office of Basic Energy Sciences, Chemical Sciences, Geosciences, and Biosciences Division.

REFERENCES

(1) Campos-Martin, J. M.; Blanco-Brieva, G.; Fierro, J. L. G. Hydrogen Peroxide Synthesis: An Outlook beyond the Anthraquinone Process. *Angew. Chemie - Int. Ed.* **2006**, *45*, 6962–6984.

(2) Thiel, W. R. New Routes to Hydrogen Peroxide: Alternatives for Established Processes? *Angew. Chemie - Int. Ed.* **1999**, *38* (21), 3157–3158.

(3) Ranganathan, S.; Sieber, V. Recent Advances in the Direct Synthesis of Hydrogen Peroxide Using Chemical Catalysis—A Review. *Catalysts* **2018**, *8*, 379–401.

(4) Kaynan, N.; Berke, B. A.; Hazut, O.; Yerushalmi, R. Sustainable Photocatalytic Production of Hydrogen Peroxide from Water and Molecular Oxygen. *J. Mater. Chem. A* **2014**, *2*, 13822–13826.

(5) Isaka, Y.; Kondo, Y.; Kawase, Y.; Kuwahara, Y.; Mori, K.; Yamashita, H. Photocatalytic Production of Hydrogen Peroxide through Selective Two-Electron Reduction of Dioxygen Utilizing Amine-Functionalized MIL-125 Deposited with Nickel Oxide Nanoparticles. *Chem. Commun.* **2018**, *54*, 9270–9273.

(6) Wu, X.; Zhang, X.; Zhao, S.; Gong, Y.; Djellabi, R.; Lin, S.; Zhao, X. Highly-Efficient Photocatalytic Hydrogen Peroxide

Production over Polyoxometalates Covalently Immobilized onto Titanium Dioxide. *Appl. Catal. A Gen.* **2019**, 117271.

(7) Flaherty, D. W. Direct Synthesis of H_2O_2 from H_2 and O_2 on Pd Catalysts: Current Understanding, Outstanding Questions, and Research Needs. *ACS Catal.* **2018**, *8*, 1520–1527.

(8) Chu, C.; Huang, D.; Zhu, Q.; Stavitski, E.; Spies, J. A.; Pan, Z.; Mao, J.; Xin, H. L.; Schmuttenmaer, C. A.; Hu, S.; Kim, J. H. Electronic Tuning of Metal Nanoparticles for Highly Efficient Photocatalytic Hydrogen Peroxide Production. *ACS Catal.* **2019**, *9*, 626–631.

(9) Lu, Z.; Chen, G.; Siahrostami, S.; Chen, Z.; Liu, K.; Xie, J.; Liao, L.; Wu, T.; Lin, Di.; Liu, Y.; Jaramillo, T. F.; Nørskov, J. K.; Cui, Y. High-Efficiency Oxygen Reduction to Hydrogen Peroxide Catalysed by Oxidized Carbon Materials. *Nat. Catal.* **2018**, *1*, 156–162.

(10) Viswanathan, V.; Hansen, H. A.; Nørskov, J. K. Selective Electrochemical Generation of Hydrogen Peroxide from Water Oxidation. *J. Phys. Chem. Lett.* **2015**, *6* (21), 4224–4228.

(11) Yi, Y.; Wang, L.; Li, G.; Guo, H. A Review on Research Progress in the Direct Synthesis of Hydrogen Peroxide from Hydrogen and Oxygen: Noble-Metal Catalytic Method, Fuel-Cell Method and Plasma Method. *Catal. Sci. Technol.* **2016**, *6*, 1593–1610.

(12) Samanta, C. Direct Synthesis of Hydrogen Peroxide from Hydrogen and Oxygen: An Overview of Recent Developments in the Process. *Appl. Catal. A Gen.* **2008**, *350*, 133–149.

(13) Sanderson, W. R. Cleaner Industrial Processes Using Hydrogen Peroxide. *Pure Appl. Chem.* **2000**, *72* (7), 1289–1304.

(14) Van De Velde, F.; Lourenço, N. D.; Bakker, M.; Van Rantwijk, F.; Sheldon, R. A. Improved Operational Stability of Peroxidases by Coimmobilization with Glucose Oxidase. *Biotechnol. Bioeng.* **2000**, *69* (3), 286–291.

(15) Tong, K. H.; Wong, K. Y.; Chan, T. H. A Chemoenzymic Approach to the Epoxidation of Alkenes in Aqueous Media. *Tetrahedron* **2005**, *61*, 6009–6014.

(16) Lewis, R. J.; Hutchings, G. J. Recent Advances in the Direct Synthesis of H_2O_2. *ChemCatChem* **2019**, *11*, 298–308.

(17) Menegazzo, F.; Signoretto, M.; Ghedini, E.; Strukul, G. Looking for the "Dream Catalyst" for Hydrogen Peroxide Production from Hydrogen and Oxygen. *Catalysts* **2019**, *9*, 251–283.

(18) Wilson, N. M.; Flaherty, D. W. Mechanism for the Direct Synthesis of H_2O_2 on Pd Clusters: Heterolytic Reaction Pathways at the Liquid-Solid Interface. *J. Am. Chem. Soc.* **2016**, *138*, 574–586.

(19) Landon, P.; Collier, P. J.; Carley, A. F.; Chadwick, D.; Papworth, A. J.; Burrows, A.; Kiely, C. J.; Hutchings, G. J. Direct Synthesis of Hydrogen Peroxide from H_2 and O_2 Using Pd and Au Catalysts. *Phys. Chem. Chem. Phys.* **2003**, *5*, 1917–1923.

(20) Kim, I.; Seo, M. G.; Choi, C.; Kim, J. S.; Jung, E.; Han, G. H.; Lee, J. C.; Han, S. S.; Ahn, J. P.; Jung, Y.; Lee, K. Y.; Yu, T. Studies on Catalytic Activity of Hydrogen Peroxide Generation According to Au Shell Thickness of Pd/Au Nanocubes. *ACS Appl. Mater. Interfaces* **2018**, *10*, 38109–38116.

(21) Freakley, S. J.; He, Q.; Harrhy, J. H.; Lu, L.; Crole, D. A.; Morgan, D. J.; Ntainjua, E. N.; Edwards, J. K.; Carley, A. F.; Borisevich, A. Y.; Kiely, C. J.; Hutchings, G. J. Palladium-Tin Catalysts for the Direct Synthesis of H_2O_2 with High Selectivity. *Science (80-.).* **2016**, *351* (6276), 965–968.

(22) Wilson, N. M.; Priyadarshini, P.; Kunz, S.; Flaherty, D. W. Direct Synthesis of H_2O_2 on Pd and Au_xPd_1 Clusters: Understanding the Effects of Alloying Pd with Au. *J. Catal.* **2018**, *357*, 163–175.

(23) Han, Y. F.; Zhong, Z.; Ramesh, K.; Chen, F.; Chen, L.; White, T.; Tay, Q.; Yaakub, S. N.; Wang, Z. Au Promotional Effects on the Synthesis of H_2O_2 Directly from H_2 and O_2 on Supported Pd-Au Alloy Catalysts. *J. Phys. Chem. C* **2007**, *111* (24), 8410–8413.

(24) Ouyang, L.; Da, G. J.; Tian, P. F.; Chen, T. Y.; Liang, G. Da; Xu, J.; Han, Y. F. Insight into Active Sites of Pd-Au/TiO_2 Catalysts in Hydrogen Peroxide Synthesis Directly from H_2 and O_2. *J. Catal.* **2014**, *311*, 129–136.

(25) Abate, S.; Freni, M.; Arrigo, R.; Schuster, M. E.; Perathoner, S.; Centi, G. On the Nature of Selective Palladium-Based Nanoparticles on Nitrogen-Doped Carbon Nanotubes for the Direct Synthesis of H_2O_2. *ChemCatChem* **2013**, *5*, 1899–1905.

(26) Edwards, J. K.; Solsona, B. E.; Landon, P.; Carley, A. F.; Herzing, A.; Kiely, C. J.; Hutchings, G. J. Direct Synthesis of Hydrogen Peroxide from H_2 and O_2 Using TiO_2-Supported Au-Pd Catalysts. *J. Catal.* **2005**, *236*, 69–79.

(27) Edwards, J. K.; N, E. N.; Carley, A. F.; Herzing, A. A.; Kiely, C. J.; Hutchings, G. J. Direct Synthesis of H_2O_2 from H_2 and O_2 over Gold, Palladium, and Gold-Palladium Catalysts Supported on Acid-Pretreated TiO2. *Angew. Chemie - Int. Ed.* **2009**, *48*, 8512–8515.

(28) Edwards, J. K.; Solsona, B.; N, E. N.; Carley, A. F.; Herzing, A. a; Kiely, C. J.; Hutchings, G. J. Switching off Hydrogen Peroxide Hydrogenation in the Direct Synthesis Process. *Science (80-.).* **2009**, *323*, 1037–1041.

(29) Edwards, J. K.; Pritchard, J.; Lu, L.; Piccinini, M.; Shaw, G.; Carley, A. F.; Morgan, D. J.; Kiely, C. J.; Hutchings, G. J. The Direct Synthesis of Hydrogen Peroxide Using Platinum-Promoted Gold-Palladium Catalysts. *Angew. Chemie - Int. Ed.* **2014**, *53*, 2381–2384.

(30) Guo, S.; Zhang, S.; Fang, Q.; Abroshan, H.; Kim, H. J.; Haruta, M.; Li, G. Gold-Palladium Nanoalloys Supported by Graphene Oxide and Lamellar TiO_2 for Direct Synthesis of Hydrogen Peroxide. *ACS Appl. Mater. Interfaces* **2018**, *10*, 40599–40607.

(31) Potemkin, D. I.; Maslov, D. K.; Loponov, K.; Snytnikov, P. V.; Shubin, Y. V.; Plyusnin, P. E.; Svintsitskiy, D. A.; Sobyanin, V. A.; Lapkin, A. A. Porous Nanocrystalline Silicon Supported Bimetallic Pd-Au Catalysts: Preparation, Characterization, and Direct Hydrogen Peroxide Synthesis. *Front. Chem.* **2018**, *6*, 1–13.

(32) Kanungo, S.; van Haandel, L.; Hensen, E. J. M.; Schouten, J. C.; D'Angelo, M. F. N. Direct Synthesis of H_2O_2 in AuPd Coated Micro Channels: Au in-Situ X-Ray Absorption Spectroscopic Study. *J. Catal.* **2019**, *370*, 200–209.

(33) Choudhary, V. R.; Gaikwad, A. G.; Sansare, S. D. Nonhazardous Direct Oxidation of Hydrogen to Hydrogen Peroxide Using a Novel Membrane Catalyst. *Angew. Chemie Int. Ed.* **2001**, *40* (9), 1776–1779.

(34) Abate, S.; Melada, S.; Centi, G.; Perathoner, S.; Pinna, F.; Strukul, G. Performances of Pd-Me (Me = Ag, Pt) Catalysts in the Direct Synthesis of H_2O_2 on Catalytic Membranes. *Catal. Today* **2006**, *117*, 193–198.

(35) Liu, Q.; Bauer, J. C.; Schaak, R. E.; Lunsford, J. H. Direct Synthesis of H_2O_2 from H_2 and O_2 over Pd-Pt/SiO_2 Bimetallic Catalysts in a H_2SO_4/Ethanol System. *Appl. Catal. A Gen.* **2008**, *339*, 130–136.

(36) Xu, J.; Ouyang, L.; Da, G. J.; Song, Q. Q.; Yang, X. J.; Han, Y. F. Pt Promotional Effects on Pd-Pt Alloy Catalysts for Hydrogen Peroxide Synthesis Directly from Hydrogen and Oxygen. *J. Catal.* **2012**, *285*, 74–82.

(37) Gosser, L. W.; Schwartz, J. T. Hydrogen Peroxide Production Method Using Platinun/Palladium Catalysts. 4,832,938, 1989.

(38) Ntainjua, E. N.; Freakley, S. J.; Hutchings, G. J. Direct Synthesis of Hydrogen Peroxide Using Ruthenium Catalysts. *Top. Catal.* **2012**, *55*, 718–722.

(39) Li, F.; Shao, Q.; Hu, M.; Chen, Y.; Huang, X. Hollow Pd-Sn Nanocrystals for Efficient Direct H_2O_2 Synthesis: The Critical Role of Sn on Structure Evolution and Catalytic Performance. *ACS Catal.* **2018**, *8*, 3418–3423.

(40) Ding, D.; Xu, X.; Tian, P.; Liu, X.; Xu, J.; Han, Y.-F. Promotional Effects of Sb on Pd-Based Catalysts for the Direct Synthesis of Hydrogen at Ambient Pressure. *Chinese J. Catal.* **2018**, *39*, 673–681.

(41) Sun, M.; Liu, X.; Huang, B. Dynamically Self-Activated Catalyst for Direct Synthesis of Hydrogen Peroxide (H_2O_2). *Mater. Today Energy* **2018**, *10*, 307–316.

(42) Wang, F.; Xia, C.; De Visser, S. P.; Wang, Y. How Does the Oxidation State of Palladium Surfaces Affect the Reactivity and

Selectivity of Direct Synthesis of Hydrogen Peroxide from Hydrogen and Oxygen Gases? A Density Functional Study. *J. Am. Chem. Soc.* **2019**, *141*, 901–910.

(43) Lari, G. M.; Puértolas, B.; Shahrokhi, M.; López, N.; Pérez-Ramírez, J. Hybrid Palladium Nanoparticles for Direct Hydrogen Peroxide Synthesis: The Key Role of the Ligand. *Angew. Chemie - Int. Ed.* **2017**, *56*, 1775–1779.

(44) Abate, S.; Arrigo, R.; Schuster, M. E.; Perathoner, S.; Centi, G.; Villa, A.; Su, D.; Schlögl, R. Pd Nanoparticles Supported on N-Doped Nanocarbon for the Direct Synthesis of H_2O_2 from H_2 and O_2. *Catal. Today* **2010**, *157*, 280–285.

(45) Villa, A.; Freakley, S. J.; Schiavoni, M.; Edwards, J. K.; Hammond, C.; Veith, G. M.; Wang, W.; Wang, D.; Prati, L.; Dimitratos, N.; Hutchings, G. J. Depressing the Hydrogenation and Decomposition Reaction in H_2O_2 Synthesis by Supporting AuPd on Oxygen Functionalized Carbon Nanofibers. *Catal. Sci. Technol.* **2016**, *6*, 694–697.

(46) Lee, S.; Chung, Y.-M. An Efficient Pd/C Catalyst Design Based on Sequential Ligand Exchange Method for the Direct Synthesis of H_2O_2. *Mater. Lett.* **2019**, *234*, 58–61.

(47) Witte, P. T.; Berben, P. H.; Boland, S.; Boymans, E. H.; Vogt, D.; Geus, J. W.; Donkervoort, J. G. BASF NanoSelect™ Technology: Innovative Supported Pd- and Pt-Based Catalysts for Selective Hydrogenation Reactions. *Top. Catal.* **2012**, *55* (7–10), 505–511.

(48) Witte, P. T.; Boland, S.; Kirby, F.; vanMaanen, R.; Bleeker, B. F.; deWinter, D. A. M.; Post, J. A.; Geus, J. W.; Berben, P. H. NanoSelect Pd Catalysts: What Causes the High Selectivity of These Supported Colloidal Catalysts in Alkyne Semi-Hydrogenation? *ChemCatChem* **2013**, *5* (2), 582–587.

(49) Cano, I.; Chapman, A. M.; Urakawa, A.; Van Leeuwen, P. W. N. M. Air-Stable Gold Nanoparticles Ligated by Secondary Phosphine Oxides for the Chemoselective Hydrogenation of Aldehydes: Crucial Role of the Ligand. *J. Am. Chem. Soc.* **2014**, *136* (6), 2520–2528.

(50) Edwards, J. K.; Freakley, S. J.; Lewis, R. J.; Pritchard, J. C.; Hutchings, G. J. Advances in the Direct Synthesis of Hydrogen Peroxide from Hydrogen and Oxygen. *Catal. Today* **2015**, *248*, 3–9.

(51) Gudarzi, D.; Ratchananusorn, W.; Turunen, I.; Heinonen, M.; Salmi, T. Factors Affecting Catalytic Destruction of H_2O_2 by Hydrogenation and Decomposition over Pd Catalysts Supported on Activated Carbon Cloth (ACC). *Catal. Today* **2015**, *248*, 69–79.

(52) Selinsek, M.; Deschner, B. J.; Doronkin, D. E.; Sheppard, T. L.; Grunwaldt, J. D.; Dittmeyer, R. Revealing the Structure and Mechanism of Palladium during Direct Synthesis of Hydrogen Peroxide in Continuous Flow Using Operando Spectroscopy. *ACS Catal.* **2018**, *8*, 2546–2557.

(53) Shimizu, K. I.; Kamiya, Y.; Osaki, K.; Yoshida, H.; Satsuma, A. The Average Pd Oxidation State in Pd/SiO_2 Quantified by L_3-Edge XANES Analysis and Its Effects on Catalytic Activity for CO Oxidation. *Catal. Sci. Technol.* **2012**, *2*, 767–772.

(54) Soldatov, A. V.; Della Longa, S.; Bianconi, A. Relevant Role of Hydrogen Atoms in the XANES of Pd Hydride: Evidence of Hydrogen Induced Unoccupied States. *Solid State Commun.* **1993**, *85* (10), 863–868..

(55) Tew, M. W.; Miller, J. T.; Van Bokhoven, J. A. Particle Size Effect of Hydride Formation and Surface Hydrogen Adsorption of Nanosized Palladium Catalysts: L_3 Edge vs K Edge X-Ray Absorption Spectroscopy. *J. Phys. Chem. C* **2009**, *113*, 15140–15147.

(56) Kubota, T.; Kitajima, Y.; Asakura, K.; Iwasawa, Y. Pd L_3 Edge XANES Spectra of Supported Pd Particles Induced by the Adsorption and the Absorption of Hydrogen. *Bull. Chem. Soc. Jpn.* **1999**, *72*, 673–681.

(57) Witjens, L. C.; Bitter, J. H.; Van Dillen, A. J.; De Jong, K. P.; De Groot, F. M. F. Pd L_3 Edge XANES Investigation of the Electronic and Geometric Structure of Pd/Ag-H Membranes. *Phys. Chem. Chem. Phys.* **2004**, *6*, 3903–3906.

(58) Lien, C. H.; Medlin, J. W. Control of Pd Catalyst Selectivity with Mixed Thiolate Monolayers. *J. Catal.* **2016**, *339*, 38–46.

(59) Pang, S. H.; Schoenbaum, C. A.; Schwartz, D. K.; Medlin, J. W. Directing Reaction Pathways by Catalyst Active-Site Selection Using Self-Assembled Monolayers. *Nat. Commun.* **2013**, *4*, 1–6.

(60) Kahsar, K. R.; Schwartz, D. K.; Medlin, J. W. Liquid- and Vapor-Phase Hydrogenation of 1-Epoxy-3-Butene Using Self-Assembled Monolayer Coated Palladium and Platinum Catalysts. *Appl. Catal. A Gen.* **2012**, *445–446*, 102–106.

(61) Adams, J. S.; Chemburkar, A.; Kulkarni, G.; Priyadarshini, P.; Karim, A. M.; Neurock, M.; Flaherty, D. W. Solvents Facilitate Proton-Electron Transfer in Direct Synthesis of H_2O_2. In *2019 North American Catalysis Society Meeting*; Chicago, 2019; Vol. 26.

(62) Coan, P. D.; Ellis, L. D.; Gri, M. B.; Schwartz, D. K.; Medlin, J. W. Enhancing Cooperativity in Bifunctional Acid – Pd Catalysts with Carboxylic Acid-Functionalized Organic Monolayers. *J. Phys. Chem. C* **2018**, *122* (12), 6637–6647.

(63) Schoenbaum, C. A.; Schwartz, D. K.; Medlin, J. W. Controlling Surface Crowding on a Pd Catalyst with Thiolate Self-Assembled Monolayers. *J. Catal.* **2013**, *303*, 92–99.

For Table of Contents Only